

**Detection of the  $Z'$  vector boson in the jet decay mode ( $Z' \rightarrow q\bar{q}$ ) $(g \rightarrow jj)$ .  
Resolution and pile-up studies**

**A. Henriques<sup>1,2</sup>, L. Poggiali<sup>1</sup>**

<sup>1</sup> Cern, Geneva, Switzerland, <sup>2</sup> LIP, Lisbon, Portugal

**Abstract**

*We report on the feasibility of detecting the  $Z'$  vector boson in the 2-jet decay mode. A range of masses from 1 to 5 TeV is analysed. The effect of the jet energy resolution of the calorimeter and the pile-up on the jet mass resolution is studied for  $m_{Z'}=2$  TeV and intrinsic width  $\Gamma_{Z'}=63$  GeV. We conclude that the energy resolution of the calorimeter and the pile up are important factors in the jet mass resolution of the signal. It is possible to observe the boson  $Z'$  in the di-jet decay mode at high luminosities ( $L \geq 10^{34} \text{ cm}^{-2} \text{ s}^{-1}$ ) up to 3-4 TeV with a good detector energy resolution ( $\sigma/E-50/\sqrt{E} \oplus 2-3\%$ ) in presence of pile-up despite of the high QCD background levels. The mass resolution obtained for the signal with the jet decay mode is not competitive with the  $e^+e^-$  decay mode.*

**1 - Motivation**

The existence of new neutral and charged vector bosons ( $Z', W^{\pm'}$ ) at the TeV energy scale is predicted by several theoretical models that can be divided in two groups [1]:

- Minimal extensions of the standard model attempting to unify interactions, and are characterized by elementary Higgses: E6 models, left-right models, extended gauge models, etc.

- More drastic models involving a different mechanism for the electroweak symmetry breaking like Bess models, models with composite W and Z bosons and technicolor models.

These models differ by the  $Z'$ -couplings to fermions. In the extended gauge model used in this study to generate the signal events, the  $Z'$  couples to fermions as in the standard model and to ordinary W and Z. The total  $Z'$ -width increases linearly with the mass of the  $Z'$  and the branching ratios into fermions are similar to those of ordinary  $Z^0$  into fermions. The total  $Z'$  width in the extended gauge model is about 3% of the  $Z'$  mass, see fig.1a, where it is show the  $\Gamma_{Z' \text{ total}}$  as a function of the  $Z'$  mass considering different theoretical models[1]. An E6  $Z'$  would have a production cross section about 3 to 5 times smaller depending on the mixing angle.

For an integrated luminosity of  $10^5 \text{ pb}^{-1}$  the discovery limits for the  $Z'$  of E6 model origin or isoscalar composite bosons are around 4TeV [2], i.e. in a range adequate to be observable at LHC and SSC colliders. Before data taking will start at LHC either mixing of the  $Z^0$  with  $Z'$  at LEP1 will be observed, or a limit on a possible mixing smaller than 1% will have been set. At LEP200 there will be a sensitivity to masses of new vector bosons, and from precision measurements it will be possible to exclude certain models.

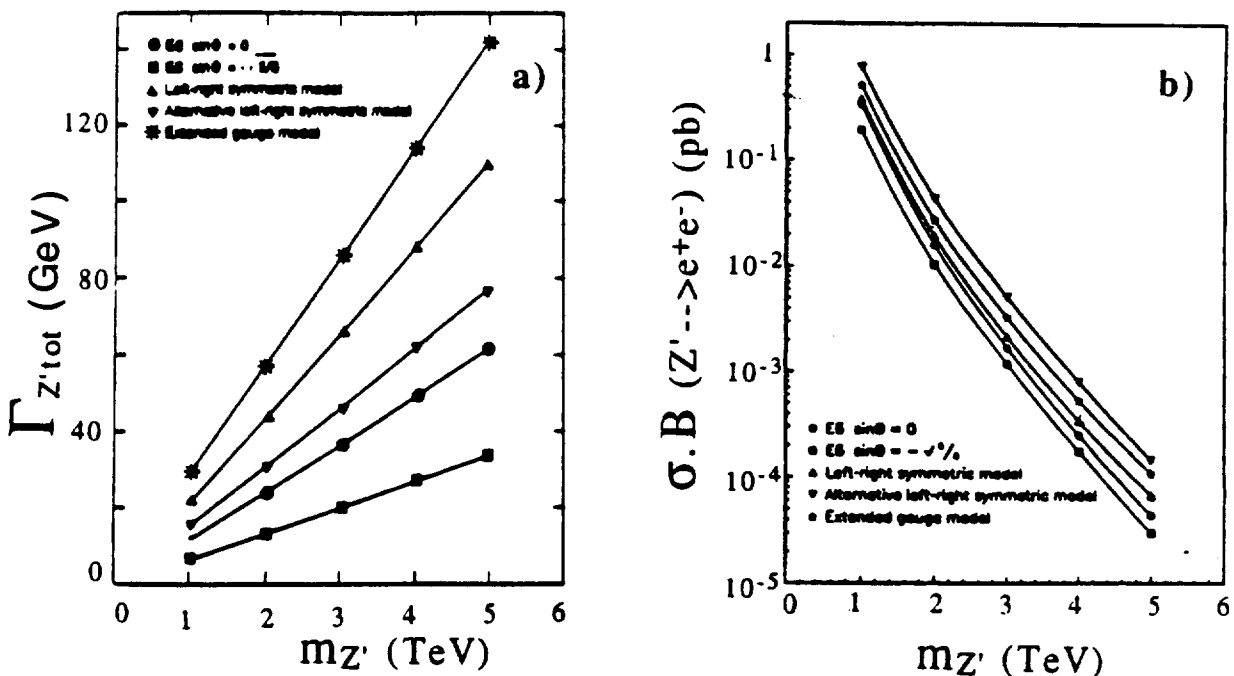


Fig. 1- (a)  $\Gamma_{\text{total}}(Z')$  and (b)  $\sigma \cdot B$  as a function of the  $Z'$  mass for different theoretical models (from reference[1]).

Among the possible decay modes of the  $Z'$ <sup>\*</sup> :

1) $Z' \rightarrow e^+ e^-$	(B.R.=3.21%)
2) $Z' \rightarrow \mu^+ \mu^-$	(B.R.=3.36%)
3) $Z' \rightarrow q\bar{q}(g) \rightarrow jj$	(B.R.=70.9%)
4) $Z' \rightarrow W^+ W^-$ ( $W^+ W^- \rightarrow l\nu jj$ ; $W^+ W^- \rightarrow e^+ e^- jj$ )	
5) $Z' \rightarrow ZH$ ( $ZH \rightarrow ZWW$ ; $ZH \rightarrow ZZZZ$ )	

most of the simulation studies for the  $Z'$  boson done so far have been concentrated in the leptonic decay mode 1) and 2), since these are the cleaner channels to detect the signal. The background levels are negligible compared to the signal. Results from [2], and [4] shown that the  $e^+ e^-$  mode provides the best signal mass resolution. A mass limit for the detection of the  $Z'$  in the leptonic mode was found to be 4TeV, considering as a limit of detection to have at least 10 events per year at  $L=10^{34} \text{cm}^{-2} \text{s}^{-1}$  including efficiency cuts .

Incomplete simulation studies done so far on the jet decay mode of the  $Z'$  (not including any jet algorithm or fragmentation [3] and [4]), conclude that in the future pp colliders (LHC, SSC) the QCD background level is enormous, typically  $10^4$  times the jet signal from the  $Z'$ , which makes impossible or very difficult to observe the signal. Nevertheless it is important to study in quite some detail this decay mode for energies ranges where the leptonic decay mode is compromised due to the low number of events produced ( $4 \text{TeV} \leq m_{Z'} < 5 \text{TeV}$ ). On the other hand the study of the jet decay mode in the same range of energies already covered by the leptonic decay mode is important because one can determine coupling constants and test theoretical models.

Understanding the effect of the energy resolution of the detector and the presence of pile-up on the jet mass resolution at the TeV energy scale are important for setting constraints on the hadronic calorimeter performance even for other physics where jets have to be detected at this energy scale (e.g compositeness).

This report is divided in 6 sessions. Section 2 explains the procedure of the analysis. A monte Carlo generator is used to simulate the signal and QCD background events. The simulation of the detector and the jet algorithm used are described. In section 3 are presented the selection cuts in order to increase the statistical

---

\* In this study it was considered the same branching ratios as for the  $Z^0$  boson.

significance keeping a reasonable number of signal events. In section 4 are studied the various factors that are affecting the mass resolution of the signal for a  $Z'$  boson decaying in the jet decay mode, namely the effect of the jet algorithm, the presence of pile up, the effect of the fragmentation (on the mass resolution and on the low mass tail present on the reconstructed invariant mass distribution). The effect of the jet energy resolution of the hadronic calorimeter on the mass resolution is also studied. The results presented on sessions 4 concern to the  $Z'$  boson of 2TeV with a natural width  $\Gamma_{Z'}$  equal to 63GeV. In section 5 is studied the feasibility of detecting the  $Z'$  vector boson in the jet decay mode for  $m_{Z'} = 1, 1.5, 2, 3, 4$  and 5TeV for integrated luminosities from  $10^4 \text{ pb}^{-1}$  to  $2.10^5 \text{ pb}^{-1}$ . Conclusions are given in section 6.

## 2- Procedure

### *Generation of the signal and QCD background*

The signal of the vector boson  $Z' \rightarrow q\bar{q}(g) \rightarrow jj$  and QCD background were generated using the Pythia 5.4 Monte Carlo generator [5] assuming a minimal SM extension model for the signal. The extended gauge model used in this study to simulate the  $Z'$  signal gives the second highest values for the signal cross sections expected. This can be shown in fig. 1b where are plotted the values of  $\sigma \cdot B$  as a function of the  $Z'$  mass for the leptonic decay mode  $Z' \rightarrow e^+e^-$  considering different theoretical models [1].

Events were generated to study  $m_{Z'} = 1, 1.5, 2, 3, 4$  and 5TeV. In table 1a and fig. 2 are presented the cross sections of the generated signal events and on table 1b the generated QCD background events. A kinematic cut was applied in the  $m_{q\bar{q}}$  generated for the signal and background to reject events with  $m_{q\bar{q}} < m_{Z'}$ . This eliminates a big fraction of non interesting  $q\bar{q}$  final state events of the type:



with a final reconstructed jet mass far from the interesting  $m_{Z'}$  region. Two additional cuts on the generation of the background events were applied:

-  $P_{qT} > P_{T\text{cut}}$ . The value of  $P_{T\text{cut}}$  applied in the generation of the background for the various  $Z'$  masses is indicated in table 1 (column 5). This cut is justified because the  $Z'$  is produced centrally, and the jets will be produced back to back with a high transverse momenta.

- It was imposed the condition  $|\eta| \leq \eta_{\text{cut}} = 2.1$  for the same reason as above. This condition enables to reject already at the generation a considerable fraction of QCD background events that are produced at large rapidities.

a) Signal events generated				
$m_{Z'}$ (TeV)	$\Gamma_{Z'}$ (GeV)	$\sigma.B$ (pb)	# events generated	Conditions applied in the generation
1	31	13.9	1573	$m > 500\text{GeV}$
1.5	47	3.6	1546	$m > 500\text{GeV}$
2	63	0.71	5000	$m > 1000\text{GeV}$
3	95	0.073	1194	$m > 2000\text{GeV}$
4	127	$1.0 \times 10^{-2}$	1139	$m > 3000\text{GeV}$
5	159	$1.6 \times 10^{-3}$	1861	$m > 4000\text{GeV}$

b) QCD background events generated			
for $m_{Z'}$ of (TeV)	$\sigma.B$ (pb)	# events generated	Conditions applied in the generation
1	$1.1 \times 10^5$	4500	$ \eta  \leq 2.1 ; P_T \geq 150\text{GeV} ; m > 500\text{GeV}$
1.5 and 2	5300	30000	$ \eta  \leq 2.1 ; P_T \geq 300\text{GeV} ; m > 1000\text{GeV}$
3	200	1856	$ \eta  \leq 2.1 ; P_T \geq 500\text{GeV} ; m > 2000\text{GeV}$
4	24	1877	$ \eta  \leq 2.1 ; P_T \geq 600\text{GeV} ; m > 3000\text{GeV}$
5	3.3	1861	$ \eta  \leq 2.1 ; P_T \geq 800\text{GeV} ; m > 4000\text{GeV}$

Table 1- Values for the cross sections of the generated (a) signal and (b) and QCD background events. Events were generated to study  $m_{Z'} = 1, 1.5, 2, 3, 4, 5\text{TeV}$ .

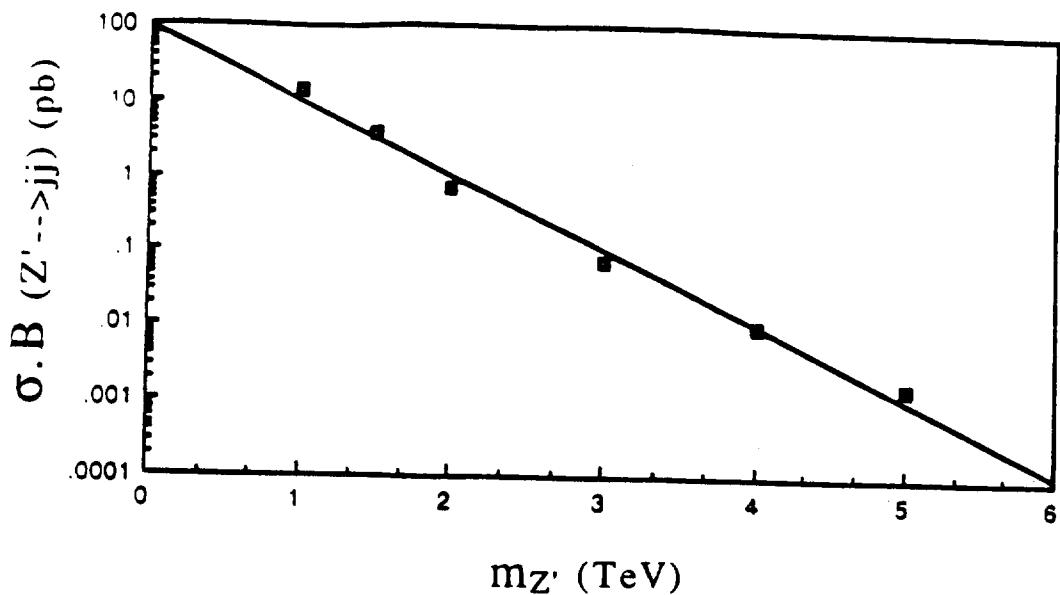


Fig. 2- *Cross section time branching ratio of the dijet decay mode from the extended gauge model as a function of the Z' mass. The conditions applied at the generation level are given in table 1a.*

The precision of this study will be limited by the big statistical errors on the background. For the most favourable case (2TeV) only  $\sim 0.06\%$  of the expected number of background events expected in a real experiment at the LHC, for an integrated luminosity of  $10^4 \text{ pb}^{-1}$  have been generated. The number of generated signal events is approximately the same as the number expected for the same integrated luminosity.

From the values of the cross sections given for the signal and QCD background given in table 1, without making any additional cut optimization we conclude that the signal to background ratio is of the order of  $10^{-4}$  level, which makes very difficult a priori to observe the signal in these conditions.

#### *Detector simulation*

This study has been done at the particle level without any Geant simulation for the shower development. The calorimeter covering  $|\eta| \leq 3$  and  $0 < \phi < 2\pi$  was divided in cells of  $\Delta\phi \times \Delta\eta = 0.06 \times 0.126$ . Particles entering a cell deposited their total energy in this cell. After applying a jet algorithm, an overall jet energy resolution has been applied  $\sigma/E = a/\sqrt{E} + b$  (see section 4.4).

### Jet Algorithm

To reconstruct the jets it was used a standard jet algorithm collecting energies in cells around a local maximum within a cone of half-angle  $\Delta R_{\text{cone}} = \sqrt{\Delta\phi^2 + \Delta\eta^2}$  has been used. The effect of the cone size on the reconstructed jet mass resolution will be studied in section 4. Values of  $\Delta R_{\text{cone}}$  from 0.4 to 1.8 have been tried as discussed in section 4.

### 3- Event selection conditions

To detect the signal under such enormous background levels ( $S/B \sim 10^{-4}$ ) there are two necessary conditions: to know precisely the background over a wide region in mass and to have a large value of the statistical significance ( $S/\sqrt{B} \gg 1$ ). To obtain this we have to optimize several cuts in order to keep an acceptable signal level and a precise knowledge of the background. In fig. 1a and 1b it is shown respectively the  $\eta$  distribution and the minimum  $P_T$  of the quarks of the generated signal ( $m_{Z'} = 2\text{TeV}$ ) for an integrated luminosity of  $10^4 \text{pb}^{-1}$  before additional cuts. For example for the  $Z'$  boson of 2TeV mass a final low  $P_T$  cut of 300GeV was chosen which will introduce a bias on the background for masses smaller than  $2 \times 300 / \text{sh}|\eta|_{\text{max}}$ . A reduction of the background to signal ratio has been obtained by playing on the  $\eta_{\text{cut}}$ .

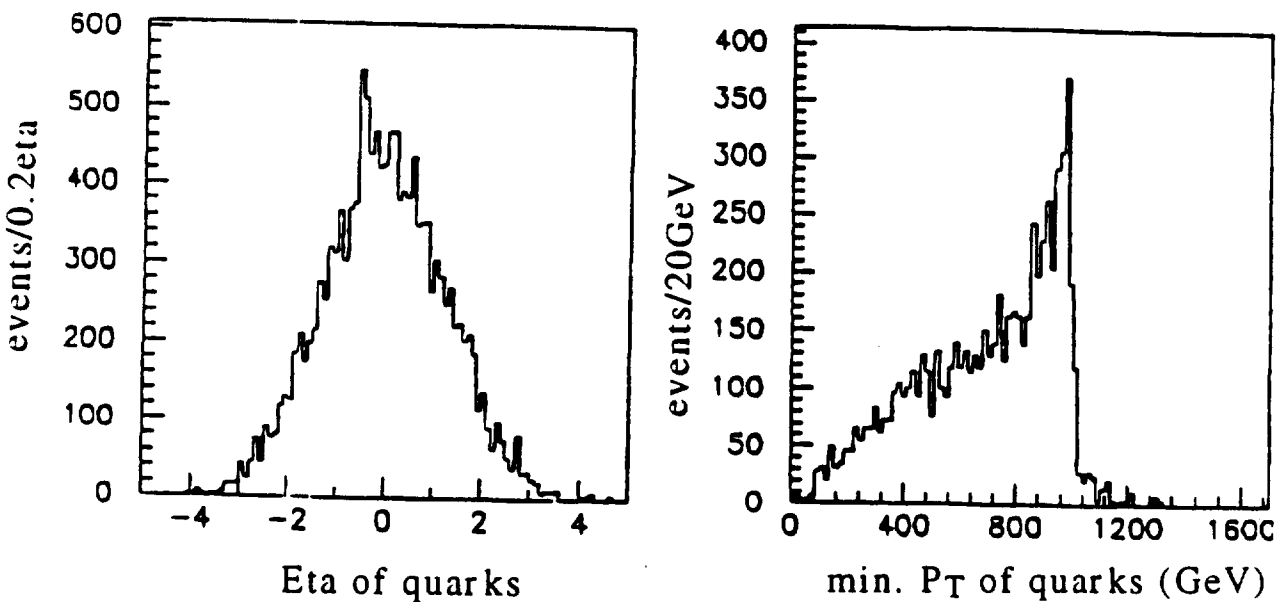


Fig. 3- Acceptance cuts shown for the  $Z'$  signal ( $m_{Z'} = 2\text{TeV}$ ,  $\Gamma = 63\text{GeV}$ ).

Table 2 presents the results for the efficiency on detecting the signal and background for a  $Z'$  mass of 2TeV ( $\Gamma_{Z'}=63\text{GeV}$ ) as a function of the  $\eta_{\text{cut}}$  when a  $\text{pjetTcut}$  of 300GeV was applied. Only events within  $\sim\pm 2\Gamma$  of the  $Z'$  invariant mass peak are taken into account to calculate the acceptance levels and the statistical significance. The fourth column of table 3 gives the values of the mass window for each  $Z'$  mass.

$\eta_{\text{cut}}$	signal year	backg year ( $\times 10^5$ )	signal (%)	back. (%)	$\frac{S}{B}$ ( $\times 10^{-3}$ )	$\frac{S}{\sqrt{B}}$
$\eta_{\text{cut}}=2.0$	2262	13	100	100	1.8	2.0
$\eta_{\text{cut}}=1.8$	2062	9	91	69	2.3	2.2
$\eta_{\text{cut}}=1.5$	1771	5	78	38	3.3	2.4
$\eta_{\text{cut}}=1.3$	1401	3.3	62	25	4.3	2.5
$\eta_{\text{cut}}=1.0$	1003	1.8	44	14	5.7	2.4
$\eta_{\text{cut}}=0.8$	648	0.8	29	6	9	2.4
$\eta_{\text{cut}}=0.5$	294	0.1	13	0.8	30	2.9

Table 2- Efficiency values for the signal and background produced for an integrated luminosity of  $10^4\text{pb}^{-1}$  as a function of  $\eta_{\text{cut}}$ , keeping  $\text{PTcut}=300\text{GeV}$ . The data presented in this table considered only the events within a mass window of  $\pm 120\text{GeV}$  ( $\sim\pm 2\Gamma$ ) around the  $Z'$  invariant mass peak.

The cut on  $|\eta_{\text{jetmax}}|$  affects more the background than the signal. The final cuts applied for  $Z'$  bosons of 1, 1.5, 2, 3, 4, and 5TeV mass, as well as the mass acceptance imposed by the cuts applied are given in Table 3. A value of  $\eta_{\text{cut}}$  smaller than 1 was not studied due to the severe statistical limitation on the number of generated background events. Nevertheless a value of  $\eta_{\text{cut}}=0.5$  would increase the signal to background ratio by a factor of  $\sim 10$  with respect to  $\eta_{\text{cut}}=1.0$ . To confirm that the acceptance values given in table 2 for the background for small values of  $\eta_{\text{cut}}$  ( $\eta_{\text{cut}} \leq 1.0$ ) are not being affected by the poor statistics inside the mass window choosed to compare the reduction of the background level as a function of  $\eta_{\text{cut}}$  (table 2) with the reduction of the cross section of the background generated with a cut on  $\eta$  equal to 2.1, 1.0 and 0.5, keeping always the same  $\text{PTcut}=300\text{GeV}$ . The values obtained with the *Phythia* generator using the extended gauge model are presented in

table 4. The reduction of the cross section observed in table 4 as a function of the cut on  $\eta$  applied at the generation level is compatible with the reduction of the number of background events within the window mass of  $\pm 120\text{GeV}$  when the same cut on  $\eta$  is applied at the jet algorithm level (table 2, column 5).

$m_{Z'}$ (TeV)	$\eta_{cut}$	$P_{Tcut}$ applied to the background (GeV)	mass window (GeV)	unbiased jet jet range (GeV)
1	1.0	150*	$\pm 62$	$m \geq 462$
1.5	1.0	300	$\pm 94$	$m \geq 926$
2	1.0	300	$\pm 120$	$m \geq 926$
3	1.0	500	$\pm 190$	$m \geq 1543$
4	1.0	600	$\pm 254$	$m \geq 1852$
5	1.0	800	$\pm 320$	$m \geq 2469$

Table 3- Final conditions applied to the generated events for the signal and background for  $m_{Z'}=1, 1.5, 2, 3, 4$  and  $5\text{TeV}$ . The unbiased mass region is given by  $m \geq 2P_{tcut}/\sin\theta_{cut}$  where  $\eta_{cut}=1$  corresponds to  $\theta_{cut}=40.4^\circ$ .

$\eta_{cut}$	$\sigma, B$ (pb)
2.1	5300
1.0	1098
0.5	160

Table 4- Values of the cross section times the branching ratio obtained with the Pythia monte Carlo generator for the QCD background generated for the  $Z'$  boson of  $2\text{TeV}$  mass in the jet decay mode with different values of  $\eta_{cut}$  applied at the generation level, keeping constant a  $P_{Tcut}=300\text{GeV}$ .

#### 4- Jet mass resolution studies

The di-jet mass resolution  $\sigma_m/m$  depends on several factors namely on the jet algorithm, on additional energy fluctuation due to pileup and on the calorimeter performance. All these parameters are studied in this section.

\* The trigger rate at level 1 can be too high for this cut. It has to be investigated.

#### 4.1- Effect of the jet algorithm

##### *Cone size optimization*

The cone size  $\Delta R_{\text{cone}} = \sqrt{\Delta\phi^2 + \Delta\eta^2}$  used to reconstruct jets (see section 2) affects the reconstructed mass resolution in two opposite ways:

- 1) If very narrow cones are applied particles from the fragmentation process emitted at large aperture angles with respect to the parent parton direction will not be detected, yielding namely a low mass tail in the invariant jet mass distribution, and a degradation of the mass resolution.
- 2) The use of wide cones gives as a consequence the collection of particles not only assigned to the jet originated from the  $Z'$  signal, but also from the underlying event. In addition the minimum bias events present in LHC experiments working at high luminosities ( $L \geq 10^{33} \text{ cm}^{-2} \text{ s}^{-1}$ ) will be superimposed to the collected signal. This will produce a degradation of the jet mass resolution.

These two effects are opposite so an optimization of the cone size where the energy of the cells is summed has been optimized to obtain the best jet mass resolution. This optimisation has been done in absence of minimum bias events (working luminosity of  $10^{33} \text{ cm}^{-2} \text{ s}^{-1}$ ) and adding 10 minimum bias events ( $L = 10^{34} \text{ cm}^{-2} \text{ s}^{-1}$ ) to the signal and to the background for the  $Z'$  boson of 2TeV mass ( $\Gamma = 63 \text{ GeV}$ ) using an ideal detector ( $\sigma_E/E = 0$ ).

Fig. 4 shows the invariant jet mass distribution of the signal for  $\Delta R_{\text{cone}} = 0.4$ , 0.7 1.0, 1.4 and 1.8 in absence of minimum bias events. One observes an increase of the mean response with increasing cone size as expected. The narrow cones present a big low mass tail resulting from the loss of fragmentation products, and it is reduced when the cone size is increased.  $\Delta R_{\text{cone}} = 0.7$  gives the best jet mass resolution , see fig. 5 where the values of the jet mass resolution ( $\sigma_m/m$ ) as a function of the cone size in absence of minimum bias events (square points) are presented. The value of  $\sigma_m$  taken is  $\text{FWHM}/2.35$ . A worsening of the jet mass resolution is observed for narrower and wider cones.  $\Delta R_{\text{cone}} = 0.7$  is still the optimum cone size for a luminosity of  $10^{34} \text{ cm}^{-2} \text{ s}^{-1}$  (♦ points in fig 5). The degradation of the mass resolution when 10 minimum bias events are added will be discussed in section 5.

#### 4.2- Effect of the fragmentation

It is important to check if the low mass tail remaining in the dijet mass distribution for the optimized cone of 0.7 (fig. 4b), and the slightly larger width of the dijet mass distribution (FWHM=80-100GeV, see fig. 4b) compared to the intrinsic width of the  $Z'$  boson considered in the model ( $\Gamma_{Z'}=63\text{GeV}$ ) comes only from the jet algorithm, or has also some contribution from fragmentation effects. The results shown have been obtained assuming the standard model mixture of 6 quarks. The contribution of the bottom and top quarks to the signal decaying semileptonically (thus producing  $\nu$  escaping the detection) could explain partially the effect described above. This has been studied by removing the  $Z'$  signal events decay in a bottom or top quark. In fig. 6a) and 6b) it is shown respectively the dijet mass spectra for the  $Z'$  signal with all quarks contributing to the signal and when the top and the bottom quarks are removed. The number of signal events has been reduced to 60% with respect to the number of signal events when all quarks are accepted\*. The FWHM of the distribution is  $\sim 80\text{Gev}$  when  $b$  and  $t$  quarks are removed and  $80-100\text{GeV}$  when all quarks are accepted. The relative contribution of the low mass tail to the signal is slightly smaller in absence of  $b$  and  $t$  quarks, but no big differences are observed between the two curves within the precision of the mass binning (20GeV/mass bin).

Comparing the value of the FWHM for the dijet mass resolution shown in fig 6a, 6b, and the  $m_{q\bar{q}}$  distribution of the  $Z'$  signal presented in fig. 7 we still obtain in the last case a FWHM of  $80\text{GeV}$  (4 bins). We did a more refined analysis making a fit with a Breit Wigner function to the  $m_{q\bar{q}}$  and dijet mass distributions. The results are presented in table 5. The original intrinsic width of  $63\text{Gev}$  of the  $Z'$  boson is obtained in the  $m_{q\bar{q}}$  distribution ( $\Gamma$  from the fit is  $62\text{ GeV}$ ), but not in the dijet mass spectra even when events containing bottom and top quarks were removed. The dijet mass distribution has been fitted in two different regions: considering mostly the right part of the distribution (from  $1960\text{GeV} < m < 4000\text{GeV}$ , see fourth column of table 5) to

---

\* The relative contribution of  $b$  and  $t$  quarks expected to the  $Z'$  signal decaying in the jet decay mode is equal to:

$$(\text{BR}_{\text{bot quark}} + \text{BR}_{\text{bottom quark}})/\text{BR}_{Z' \rightarrow \text{jj}} = (15\% + 12\%)/70\% - 39\%$$

The observed reduction of events is in good agreement with the expected values.

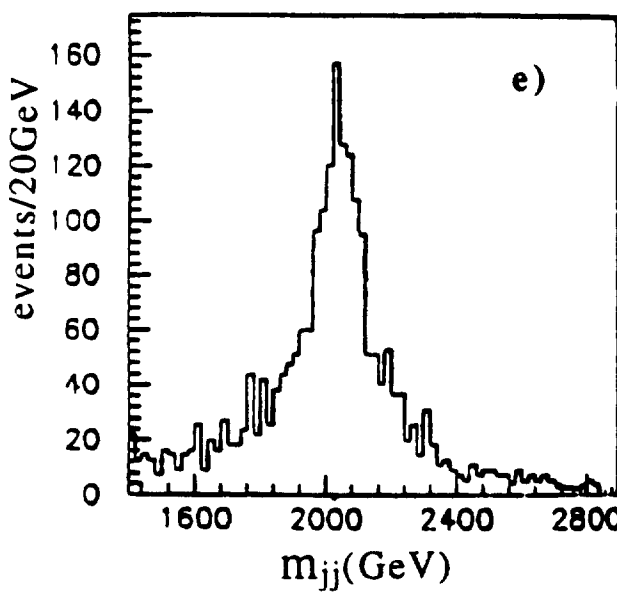
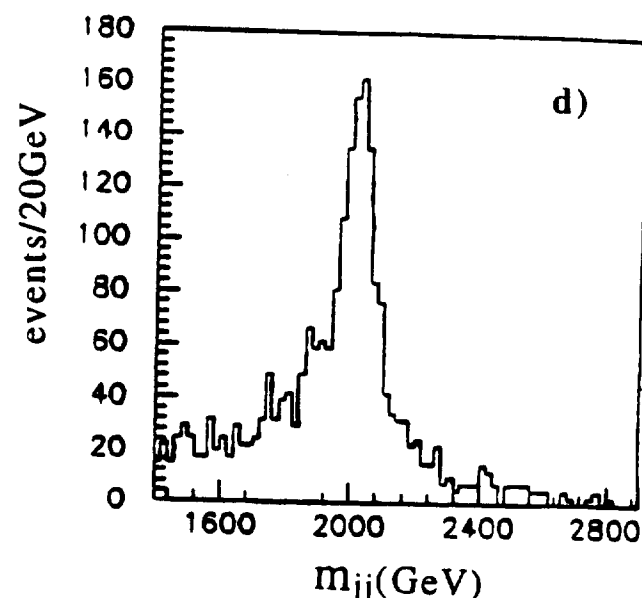
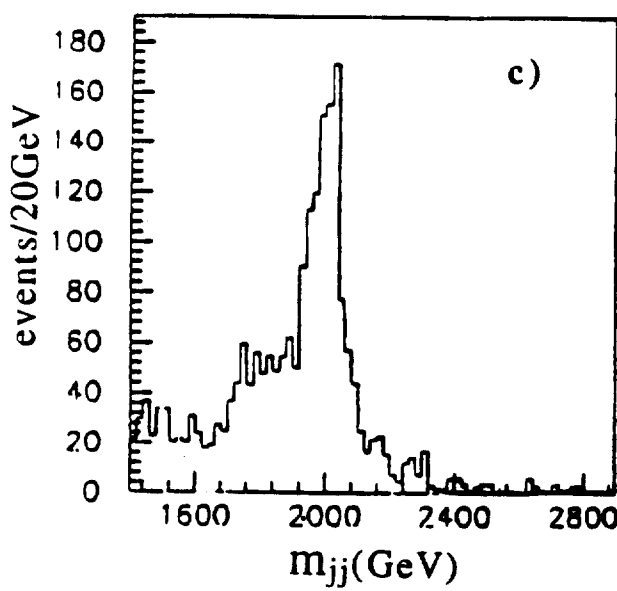
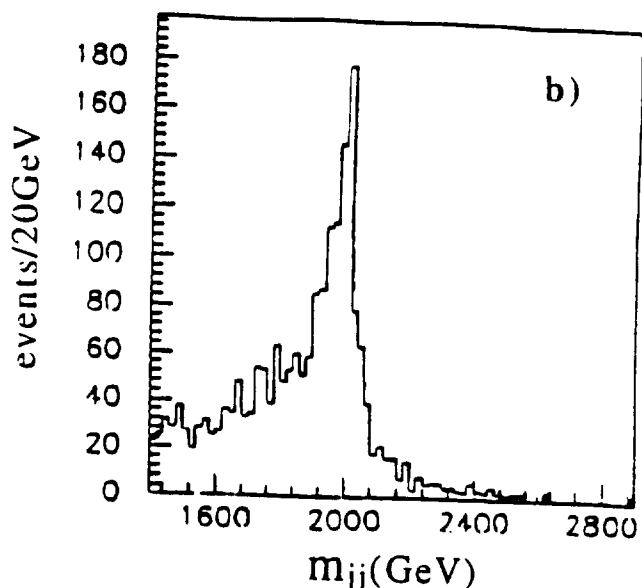
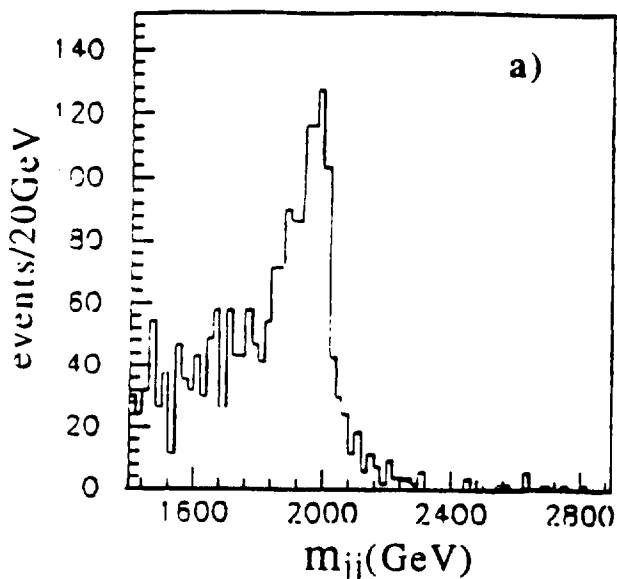


Fig. 4- Di-jet mass distribution of a  $Z'$  boson of 2 TeV mass ( $\Gamma_{Z'}=63\text{ GeV}$ ) when the cone size is equal to a) 0.4, b) 0.7, c) 1.0, d) 1.4, e) 1.8 for an ideal detector ( $\sigma/E=0$ ) for an integrated luminosity of  $10^4\text{ pb}^{-1}$ .

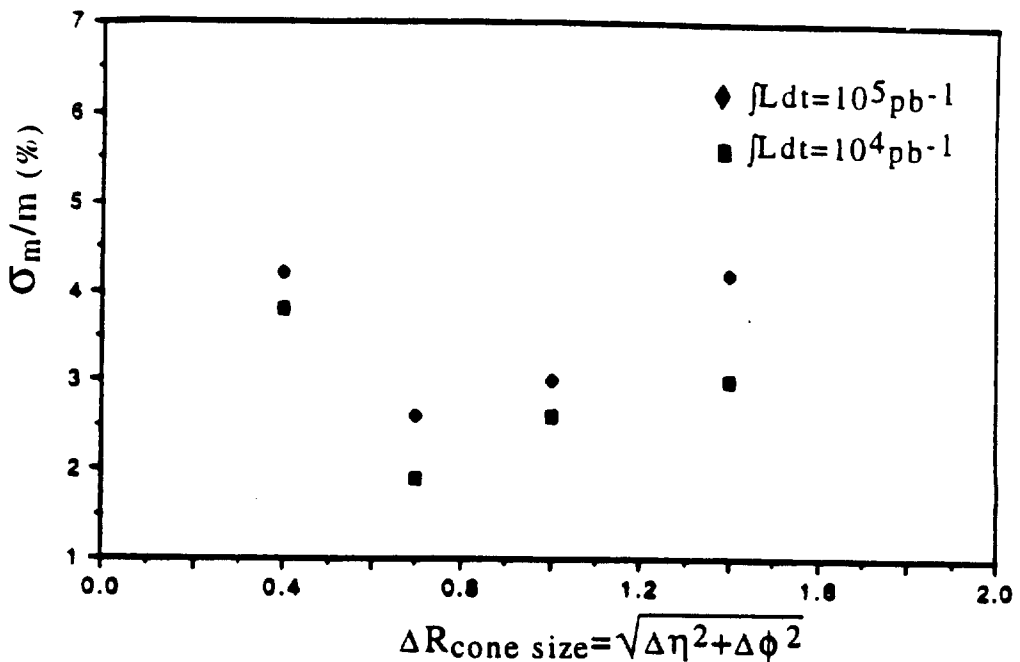


Fig. 5- Jet mass resolution of a Z' boson of 2TeV mass ( $\Gamma=63\text{GeV}$ ) as a function of the cone size for an ideal detector ( $\sigma/E=0$ ) in absence of minimum bias events (square points), and when 10 minimum bias events are added (♦ points ).

Invariant mass distribution	FWHM (GeV)	$\Gamma$ (GeV) fitted region: 1880GeV-4000GeV	$\Gamma$ (GeV) fitted region: 1960GeV-4000GeV
$m_{q\bar{q}}$	80	$63$ ( $\lambda^2=2.0$ )	$63$ ( $\lambda^2=2.0$ )
$m_{jj}$ (all quarks)	80-100	$107 \pm 5$ ( $\lambda^2=2.0$ )	$86 \pm 5$ ( $\lambda^2=1.3$ )
$m_{jj}$ (without b and t quarks)	80	$104 \pm 6$ ( $\lambda^2=2.6$ )	$81 \pm 4$ ( $\lambda^2=1.9$ )

Table 5- Results of the width of the reconstructed invariant mass distribution of the Z' boson of 2TeV mass (intrinsic width of  $63\text{GeV}$ ). It was considered different situations to obtain the value of the width: the second line was obtained without applying any jet algorithm (quark level). The third line is the normal signal obtained after applying a jet algorithm. In the fourth line the bottom and the top quark were removed to the signal.

remove the effect of geometrical losses of particles due to a finite cone size of 0.7, and taking into account a more considerable region on the left mass region of the spectra ( $1880\text{GeV} < m < 4000\text{GeV}$ , see third column of table 5). The values of the  $\lambda^2$  of the fits are not very good ( $\sim 2$ ).

The main conclusions are:

- The intrinsic width of 63GeV is not found in the invariant dijet mass distribution when the jet algorithm is applied. When the effect of fragmentation and the effect of particle losses due to the finite cone size used are eliminated by removing bottom and quark quarks from the signal and fitting the obtained spectra mostly in the right mass distribution ( $m > 1960$ TeV) a width of  $81 \pm 4$ GeV is obtained.

This means an enlargement of 30% with respect to the intrinsic width of the  $Z'$  boson due only to the jet algorithm, not taking into account the losses of particles that are produced outside of the cone. If this effect is added by fitting in a broader mass region the width found increases to  $104 \pm 6$ GeV, which means an increase of 60% width respect to the expected  $\Gamma_{Z'} = 63$ GeV. An additional increase of 6% is observed on the width due to fragmentation effects, when b and t quarks are added to the signal and making a fit in the same region it is found a final width of  $107 \pm 5$ GeV.

- The low mass tail observed in the dijet mass distribution for a size cone of 0.7 is mostly due to the losses of particles produced outside the cone. A small effect is coming from fragmentation effects. Bottom and top quarks decaying semileptonically will produce  $\mu$  and  $\nu$  not interacting in the detector.

- The combined effect of the jet algorithm (keeping the optimized cone of 0.7) and the fragmentation effect increases the the expected width of the  $Z'$  boson by a factor of 1.7. The effect of fragmentation is negligible with respect to the jet algorithm.

- The low mass tail in the dijet mass distribution turns very difficult to make a good fit in a big mass region. For this reason all the results concerning the jet resolution studies will be presented taking the FWHM directly from the distribution keeping always the same mass binning of 20GeV. This value has been chosen as a good compromise between the precision required and statistical errors.

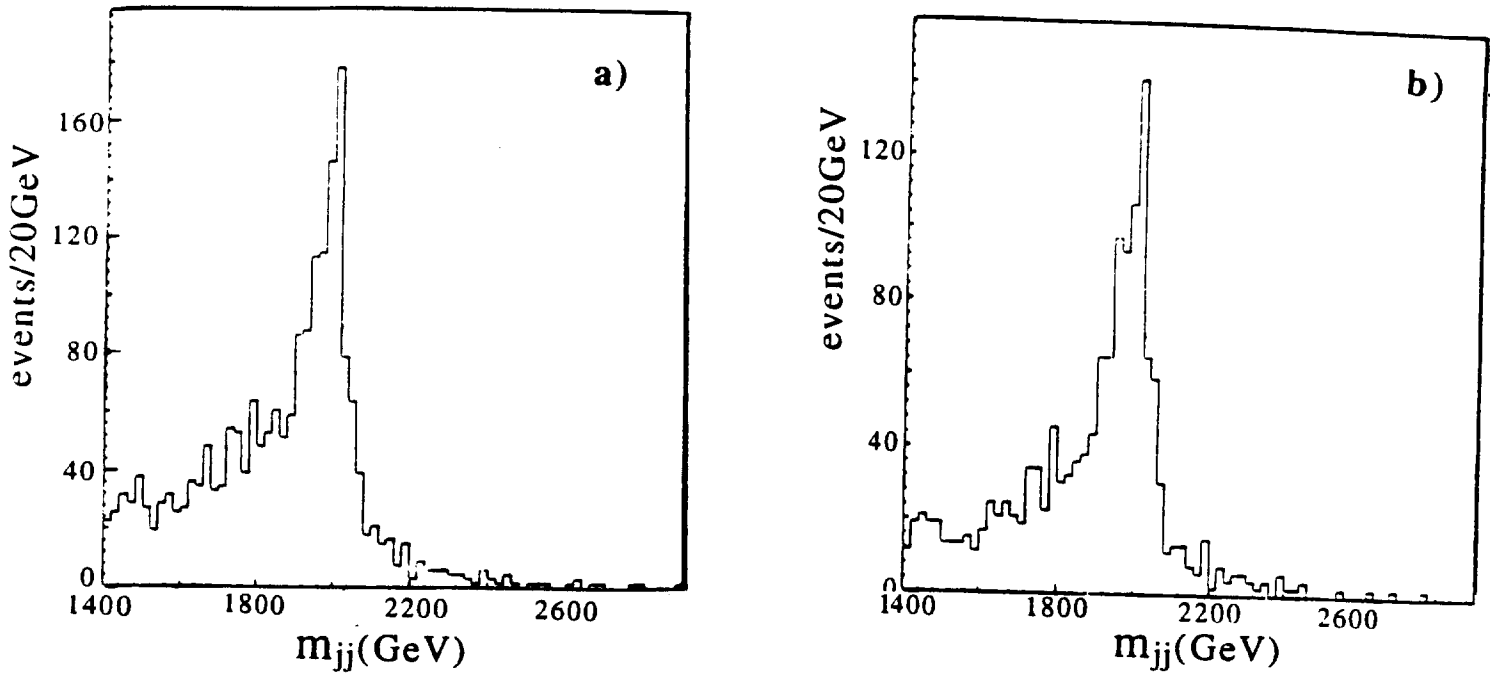


Fig. 6- Dijet mass distribution of a  $Z'$  boson of 2TeV mass ( $\Gamma=63\text{GeV}$ ) using an optimized cone of 0.7. (a) when a mixture of 6 quarks where accepted to contribute to the signal, (b) when the signal events containing bottom and top quarks where removed. It is done for an ideal detector ( $\sigma/E=0$ ) in absence of minimum bias events, for an integrated luminosity of  $10^4\text{pb}^{-1}$ .  $81\pm 4\text{GeV}$ .

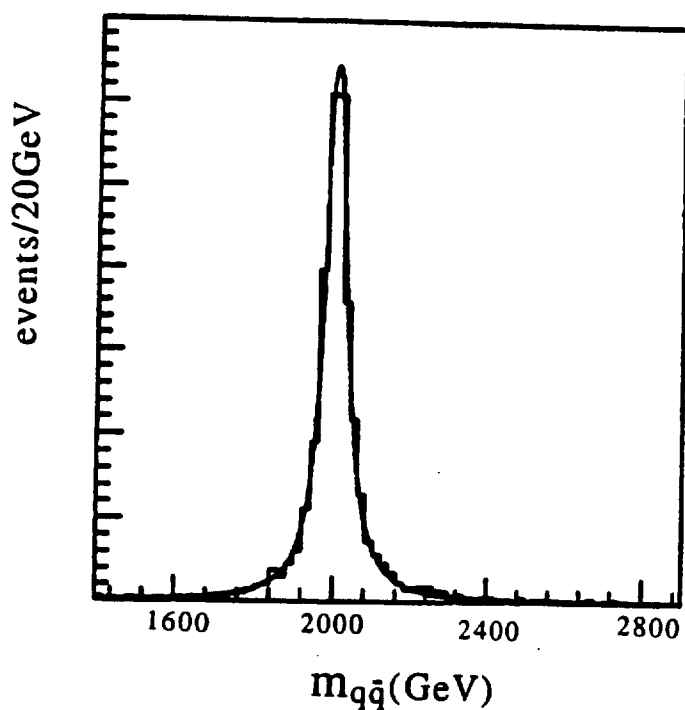


Fig. 7- Invariant  $m_{q\bar{q}}$  distribution for a  $Z'$  boson of 2TeV mass ( $\Gamma_{Z'}=63\text{GeV}$ ). The value of the FWHM is equal to 80GeV. The width obtained by making a fit with a Breit Wigner function is 62 GeV, in good agreement with the expected the expected value. It was considered an ideal detector ( $\sigma/E=0$ ) in absence of minimum bias events for an integrated luminosity of  $10^4\text{pb}^{-1}$ .

### 4.3- Effect of Pile-up

The presence of minimum bias events in the mass resolution and the statistical significance has been studied using minimum bias events generated by the Pythia generator. We assume on average  $n$  interactions to be produced per crossing for a working luminosity of  $L = n \times 10^{33} \text{ cm}^{-2} \text{ s}^{-1}$ . The particle energies from the appropriate number of such events were added to the cell energies for the signal and background events. The effect of adding 10 and 20 min. bias events to the mass resolution obtained for the  $Z'$  boson of 2TeV mass, with an intrinsic width of 63 GeV (not considering Poisson distributed around the mean value) have been studied. The results are presented in table 6. We observe a gradual shift on the reconstructed invariant mass peak to the high masses, and a degradation of the mass resolution when 10 and 20 minimum bias events are added to the signal. In the last case the resolution has deteriorated by 22-38%. The precision of the results is dependent of the mass binning used in the histograms. The mass resolution  $\sigma_m/m$  deteriorates more than expected. In fact the effect of the pileup at high luminosities on the detecting of the  $Z'$  boson at the TeV scale is expected to be negligible. Considering the use of a calorimeter fast enough to integrate the signal over one bunch crossing, the use of a cone  $\Delta R = \sqrt{\Delta\phi^2 + \Delta\eta^2} = 0.7$  produces a r.m.s. of the pile-up energy distribution  $\langle\sigma_{\text{pileup}}\rangle \geq 4.5 \text{ GeV}$  [6]. This should give a contribution of about 0.2% to the mass resolution of the  $Z'$  boson signal of 2TeV mass.

From the values of the statistical significance obtained as a function of the luminosity we conclude that the significance  $S/\sqrt{B}$  scales roughly with  $\sqrt{L}$ , and is not affected by the presence of minimum bias events.

$\int L dt (\text{pb}^{-1})$	$\Delta R_{\text{cone}}$	$\mu$	$\sigma_{\text{RMS}}$	$\sigma_m/m (\%)$	$S/\sqrt{B}$	# events at peak
$10^4$	0.7	1866	34-43	~1.8	2.4	180
$10^5$	0.7	1886	51	2.7	7.4	1540
$2 \times 10^4$	0.7	1909	55	3.1	10.1	3120

Table 6- Characteristics of the detected 2 TeV  $Z'$  signal in the dijet decay mode for different values of the integrated luminosity, for an ideal detector.  $S/\sqrt{B}$  was obtained in a mass window of  $\pm 120 \text{ GeV}$ .

It seems possible to observe the  $Z'$  boson of 2Tev mass ( $\Gamma_{Z'}=63\text{GeV}$ ) at high luminosities ( $L \geq 10^{34}\text{cm}^{-2}\text{s}^{-1}$ ) despite the extremely high level of the QCD background. This will be shown in section 5 for an integrated luminosity of  $10^5\text{pb}^{-1}$ . The combined effect of the pileup for a detector with a finite energy resolution will be discussed in the next section.

#### 4.4- Effect of the jet energy resolution of the calorimeter

Up to know all the results have been obtained assuming a calorimeter with a perfect energy resolution. It is important to see if the results shown so far are significantly affected by applying a realistic energy jet resolution for the detector.

In fig. 8 it is shown the dijet mass distribution of the  $Z'$  boson ( $m_{Z'}=2\text{ TeV}$ ,  $\Gamma_{Z'}=63\text{GeV}$ ) for different energy resolutions applied to the calorimeter:  $\sigma/E=0$ ,  $\sigma/E=30/\sqrt{E} \oplus 1\%$ ,  $\sigma/E=50/\sqrt{E} \oplus 2\%$  and  $\sigma/E=100/\sqrt{E} \oplus 4\%$ . We observe a non negligible broadening of the width of distribution and a reduction of the height of the peak when worse resolutions are applied to the calorimeter. Fig. 9 and table 7 shows the degradation of the mass resolution  $\sigma_m/m$  as a function of the number of min. bias events added to the signal considering different energy resolutions for the hadronic calorimeter.

From the results shown in fig. 8 and fig. 9 and table 7 we conclude that the energy resolution of the hadronic calorimeter plays a more important role in the mass resolution of the detected signal than the effect of pileup. The effect of the pileup at a luminosity of  $10^{34}\text{cm}^{-2}\text{s}^{-1}$  (10 m.b. events) considering an ideal or very good calorimeter ( $\sigma/E \leq 30/\sqrt{E} \oplus 1\%$  produces the same effect as a standard energy resolution calorimeter ( $\sigma/E=50/\sqrt{E} \oplus 2\%$ ) in absence of pileup. The di-jet mass resolution is in both cases equal to 3%.

A detection of jets at the TeV energy range should be more affected by the constant term of the energy resolution, dominating over the scaling term. To illustrate this effect we have frozen the scaling term to  $50\%/\sqrt{E}$  and the constant term  $c$  was changed to be 0, 1, 2, 3, 4 and 5%. This is illustrated in fig. 10 and table 8 where is shown the variation of the dijet mass resolution of the signal as a function of the constant term  $c$ . The square points in the figure corresponds to the

case where no pile up events where added to the signal and the black points when 10 m.b.e. where superimposed to the signal.

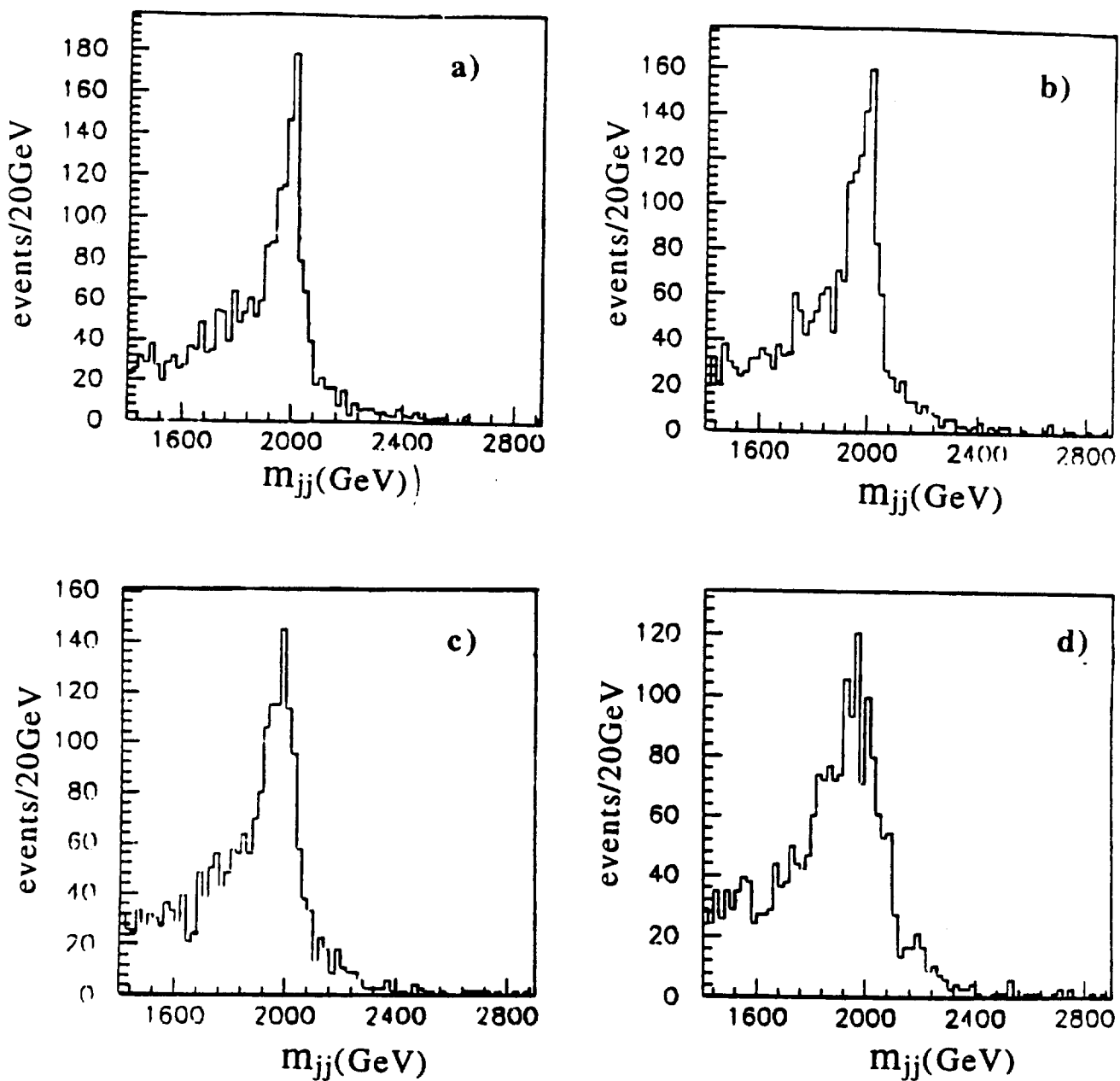


Fig. 8- Dijet mass distribution of a  $Z'$  boson of 2 TeV mass ( $\Gamma_{Z'}=63\text{GeV}$ ) for an integrated luminosity of  $10^4\text{pb}^{-1}$ , when it is applied an energy resolution to the hadronic calorimeter of a)  $\sigma/E=0$ , b)  $\sigma/E=30/\sqrt{E} \oplus 1\%$ , c)  $\sigma/E=50/\sqrt{E} \oplus 2\%$ , d)  $\sigma/E=100/\sqrt{E} \oplus 4\%$ .

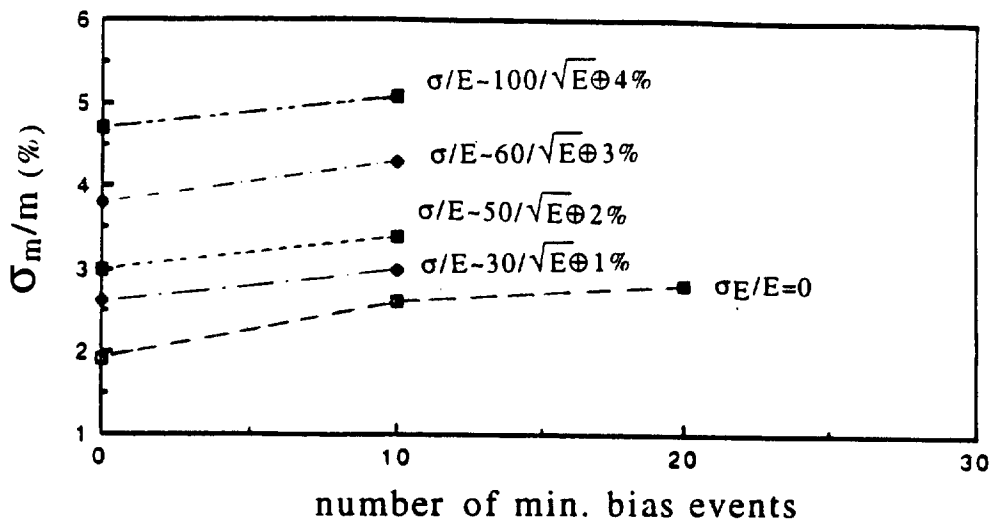


Fig. 9- Dijet mass resolution of a  $Z'$  boson of 2TeV mass ( $\Gamma_{Z'}=63\text{GeV}$ ) as a function of the number of min. bias events added to the signal. The curves presented correspond to different energy resolutions applied to the hadronic calorimeter.

$\int L dt$ ( $\text{pb}^{-1}$ )	jet energy resolution (%)	$S/\sqrt{B}$	$\sigma_{\text{RMS}}/m$ (%)	Expected $S/\sqrt{B}^*$ (%)	Expected $\sigma_{\text{RMS}}/m^{**}$ (%)
$10^4$	$\sigma/E=0$		1.9		1.9
	$\sigma/E=30/\sqrt{E} \oplus 1\%$		2.6		2.1
	$\sigma/E=50/\sqrt{E} \oplus 2\%$		3.0		2.6
	$\sigma/E=60/\sqrt{E} \oplus 3\%$		3.8		2.9
	$\sigma/E=100/\sqrt{E} \oplus 2\%$		3.4		3.2
	$\sigma/E=100/\sqrt{E} \oplus 4\%$		4.7		3.4
$10^5$	$\sigma/E=0$	7.6	2.6	7.6	2.6
	$\sigma/E=30/\sqrt{E} \oplus 1\%$	7.5	3.0	7.4	2.8
	$\sigma/E=50/\sqrt{E} \oplus 2\%$	7.4	3.4	6.8	3.2
	$\sigma/E=60/\sqrt{E} \oplus 3\%$	6.9	4.3	6.5	3.6
	$\sigma/E=100/\sqrt{E} \oplus 2\%$	7.2	3.8	6.9	3.7
	$\sigma/E=100/\sqrt{E} \oplus 4\%$	6.0	5.1	5.9	3.9

Table 7- Mass resolution of a  $Z'$  boson of 2TeV mass ( $\Gamma_{Z'}=63\text{GeV}$ ) for several hadronic energy resolution of the detector, for an integrated luminosity of  $10^4\text{pb}^{-1}$  and  $10^5\text{pb}^{-1}$ .

\* The values of  $S/\sqrt{B}$  presented for the 2TeV  $Z'$  were calculated in a fixed window mass of  $\pm 20\text{GeV}$ . Then  $\sqrt{B}$  is the same for all the values of the  $\sigma/\text{Edetector}$  assumed. Considering a gaussian distribution for the signal and the measured values of  $\sigma_m/m$  (column 4 of table 7), the expected decrease of  $S/\sqrt{B}$  is equal to the expected decrease of the signal contained on the mass window applied.

\*\*The expected  $\sigma_m/m$  is given by:  $\sigma_m/m = \sqrt{(\sigma_m/m)^2/\sigma/E=0 + (1/\sqrt{2} \times \sigma/\text{Edetector})^2}$

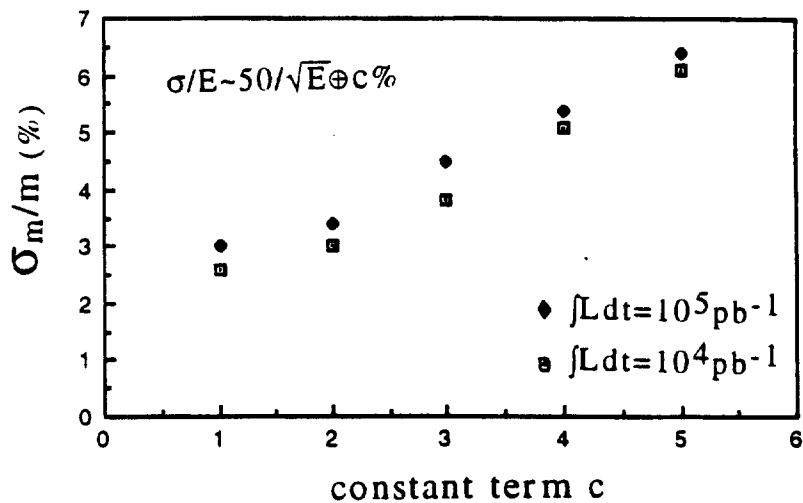


Fig. 10- Dijet mass resolution of a  $Z'$  boson of 2TeV mass ( $\Gamma_{Z'}=63\text{GeV}$ ) as a function of the constant term applied to the energy resolution of the hadronic calorimeter keeping a scaling term equal to  $50/\sqrt{E}$ . The square points corresponds to the case when no pile up events where added to the signal and the black points when 10 m.b.e. where superimposed to the signal.

$\int L dt$ ( $\text{pb}^{-1}$ )	constant term c ( $\sigma/E=50/\sqrt{E} \oplus c\%$ )	$S/\sqrt{B}$	$\sigma_{\text{RMS}}/m$ (%)
$10^4$	1		2.6
	2		3.0
	3		3.8
	4		5.1
	5		6.1
$10^5$	1	7.5	3.0
	2	7.4	3.4
	3	6.8	4.5
	4	6.1	5.4
	5	5.2	6.4

Table 8- Mass resolution of a  $Z'$  boson of 2TeV mass ( $\Gamma_{Z'}=63\text{GeV}$ ) for several hadronic energy resolution of the detector, for an integrated luminosity of  $10^4\text{pb}^{-1}$  and  $10^5\text{pb}^{-1}$ .

Comparing the effect of the pileup and the effect of the energy resolution of the hadronic calorimeter we conclude that the performance of the detector plays a more important role on the dijet mass resolution of the detected signal at the TeV energy range, namely the constant term of the energy resolution.

No study has been performed on the influence of the granularity of the hadronic calorimeter on the dijet mass resolution, but in this specific physics channel the granularity should not play an important role since the two jets are produced almost back to back. The superposition of particles from the two jets in the same cells of the calorimeter is negligible with the size cone used in the jet algorithm. In addition the pile-up events do not play a very important role on the degradation of the mass resolution.

## 5- Observability of the $Z'$ boson signal in a mass range of 1-5 TeV.

The jet spectroscopy method i.e. finding mass bumps in two jet mass distributions was already successfully demonstrated in proton antiproton collider experiments [7] for the  $W, Z$  production. The same method will be used to study the feasibility of the detection of the  $Z'$  boson signal in the jet decay mode in a mass range from 1.0 to 5 TeV. A more detailed study will be done for the case of 2 TeV mass  $Z'$  boson. The characteristics of the generated events for the signal and QCD background and the optimization of the cuts applied was presented in section 2 (see table 1 and 3). As it was already said in section 3 the detection of the signal may be very hard due to the enormous QCD background levels ( $S/B \sim 10^{-4}$ ). By consequence two conditions are needed to observe the signal: to have a precise knowledge of the background in a big mass region below and above the  $Z'$  signal, and to have a value of  $S/\sqrt{B} \gg 1$ . The selection cuts applied to the signal and the background for the various  $Z'$  masses (section 3) was such that the mass distribution is not biased in a big region around the  $Z'$  mass region (see column 5 of table 3).

Fig. 11 shows the QCD background mass spectrum around the 2 TeV mass  $Z'$  boson fitted with the best function achieved :

$$BF = e^{(A+B.m_{jj})} + e^{(C+D.m_{jj})} \quad (1.1)$$

The values of the parameters obtained are  $A = 21.76$ ,  $B = -0.496 \times 10^{-2}$  GeV,  $C = 17.03$  and  $D = -0.226 \times 10^{-2}$  GeV. The value of the qui square is equal to 1.7 per d.o.f.

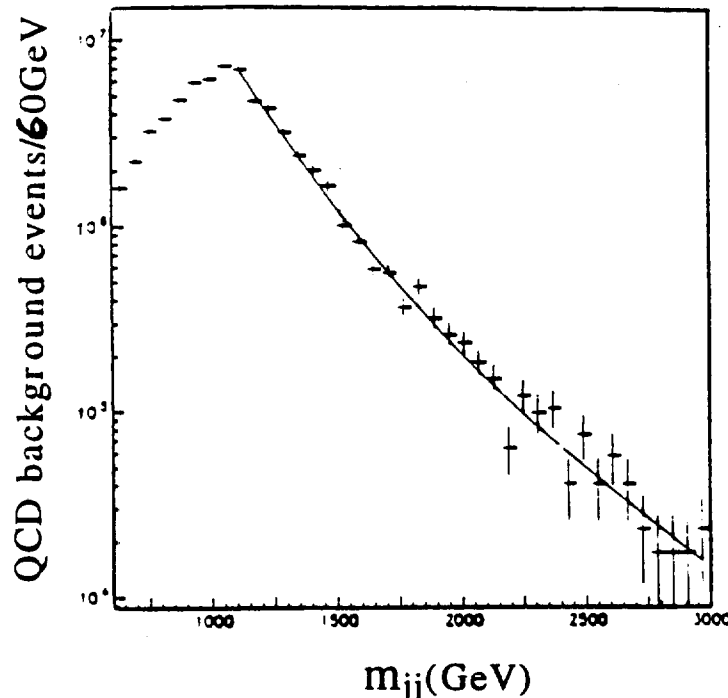


Fig. 11- *QCD Background mass spectra around the expected 2Tev mass Z' boson for an integrated luminosity of  $10^5 \text{ pb}^{-1}$ .*

In table 9 and fig. 12 we present the statistical significance and the signal to background ratio as a function of the Z' boson mass for an integrated luminosity of  $10^4 \text{ pb}^{-1}$ ,  $10^5 \text{ pb}^{-1}$  and  $2 \times 10^5 \text{ pb}^{-1}$ . We considered a jet energy resolution of  $50/\sqrt{E \oplus 2}$ .

From these results we conclude that:

- The statistical significance presents an exponential decrease with the increasing of the Z' boson mass.
- It is not possible to detect the Z' boson at low luminosity ( $L \leq 10^{33} \text{ cm}^{-2} \text{ s}^{-1}$ ).
- The statistical significance is approximately proportional to  $\sqrt{L}$ , which indicates a not significant effect of the presence of minimum bias events.
- The values obtained for the statistical significance impose a limit of detection of the Z' boson in the jet decay mode of 3TeV at high luminosity ( $L \geq 10^{34} \text{ cm}^{-2} \text{ s}^{-1}$ ). If a extra gauge boson W' was produced with about the same mass as the Z' this should enlarge the S by a factor 3 (in the Extended SM) increasing the detection limit to 4TeV.

$m_{Z'}$ (TeV)	$\Gamma_{Z'}$ (GeV)	$\int L dt$ (pb $^{-1}$ )	# min. bias events	S/B	S/ $\sqrt{B}$
1	31			$3.3 \times 10^{-3}$	10.4
1.5	47			$5.4 \times 10^{-3}$	4.2
2	63	$10^4$	0	$5.7 \times 10^{-3}$	2.4
3	95			$1.3 \times 10^{-3}$	1.2
4	127			$1.4 \times 10^{-2}$	0.5
5	159			$2.0 \times 10^{-2}$	0.2
1	31			$2.2 \times 10^{-3}$	17.9
1.5	47			$4.4 \times 10^{-3}$	13.0
2	63	$10^5$	10	$5.1 \times 10^{-3}$	7.4
3	95			$1.2 \times 10^{-3}$	3.7
4	127			$1.4 \times 10^{-2}$	1.6
5	159			$1.0 \times 10^{-2}$	0.6
2	63	$2 \times 10^5$	20	$5.0 \times 10^{-3}$	10.1

Table 9- Signal to background ratio and statistical significance for different  $Z'$  boson masses and integrated luminosities. The values were calculated in a window mass of  $\Delta m = \pm 2\Gamma_{Z'}$  using an hadronic calorimeter with a jet energy resolution of  $\sigma/E = 50/\sqrt{E} \oplus 2\%$ .

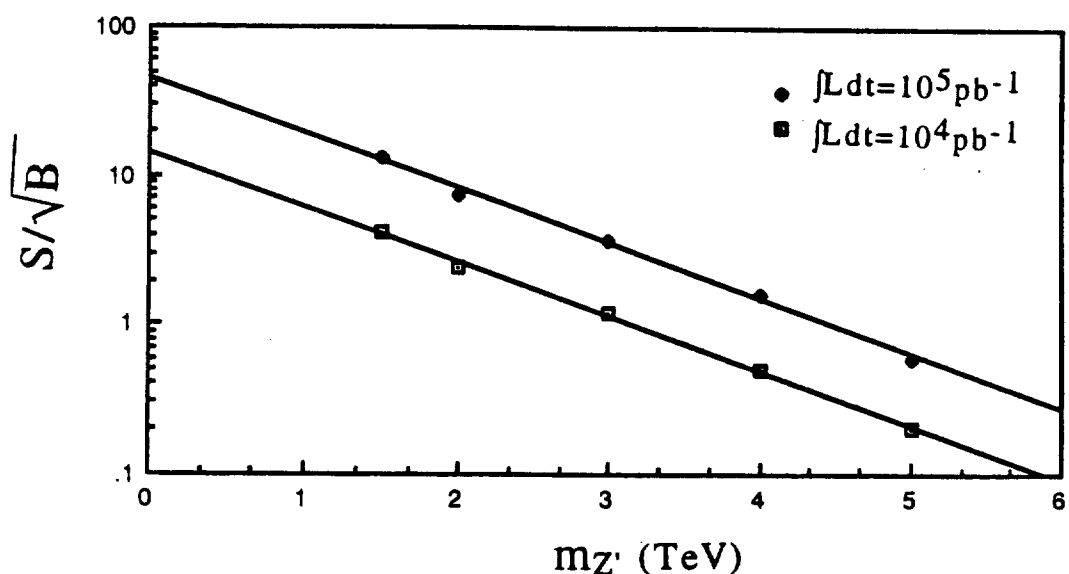


Fig. 12- Statistical significance as a function of the  $Z'$  mass obtained for an integrated luminosity of  $10^4$  pb $^{-1}$  and  $10^5$  pb $^{-1}$ . It was applied a detector with a jet energy resolution of  $\sigma/E = 50/\sqrt{E} \oplus 2\%$ .

We have simulated a real experiment for the detection of the  $Z'$  boson of 2TeV mass ( $\Gamma_{Z'}=63\text{GeV}$ ) working at an integrated luminosity of  $10^5\text{pb}^{-1}$  in presence of 10 minimum bias events. The results obtained for two experiments, considering two different values of the hadronic energy resolution of the calorimeter: a perfect calorimeter with  $\sigma/E=0$  and a crude calorimeter with  $\sigma/E=50/\sqrt{E}\oplus 2\%$  will be compared. For each case the signal mass spectrum has been fitted to a single gaussian function. The low mass tail of the spectra has not been used to make the fit. We applied a statistical fluctuation to each bin mass data point reconstructed for the signal and for the background from the fit functions described above. After this the signal and the background were summed and the obtained mass spectra was fitted with a function  $S$  which is described by:

$$S = FB(A, B, C, D) + SF(m_{Z'}, \sigma_m, N) \quad (1.2)$$

$FB(A, B, C, D)$  is the function used to describe the two jet continuum mass from the QCD processes (eq.1.1), with the values of the parameters found for the best fit (see text above). The signal function  $SF(m_{Z'}, \sigma_m, N)$  is a single gaussian function with the  $Z'$  boson mass, the mass resolution and the size  $N$  as free parameters.

The representation of the fit together with the summed mass spectra is shown in fig. 13a for a perfect hadronic energy resolution applied to the calorimeter, and in fig. 13b when a crude energy resolution of  $50/\sqrt{E}\oplus 2\%$  was applied. In the vertical scale the number of events has been weighted with the mass dependent factor  $(m/2000)^6$  to reduce the steep of the dijet mass spectrum[7]. The results of the fit and the obtained statistical significance are summarized in table 8. The observed excess of events with respect to the background fit provides a clear evidence for the signal. This is even more clear in Fig. 14a and 14b where it is shown the excess of events observed after subtracting the QCD background, for the two values of the hadronic energy resolutions applied.

The results of the dijet mass resolution and the statistical significance obtained after a real experiment simulation considering different energy resolutions for the hadronic calorimeter are presented in table 9 and fig. 12. In the ideal case, considering the use of a perfect detector the dijet mass resolution of the observed signal peak is equal to 2.6% and the statistical significance amounts to 6.8, in good

agreement with the obtained value without any experiment simulation (see section 4.4, table 7)\*. The use of a calorimeter with  $\sigma/E=50/\sqrt{E} \oplus 2\%$  on another experiment increased the mass resolution to 4.0%, which correspond to an increase of the  $\sigma_m/m$  by a factor of 1.53 with respect to the ideal detector experiment simulation, and an increase of 1.2 with respect to  $\sigma_m/m$  obtained in section 4.4 for the same energy resolution without any experiment simulation. The value of the statistical significance obtained is now 6.5 which corresponds to a decrease of ~6% with respect to the perfect calorimeter experiment close to the 10% decrease expected when a calorimeter of  $\sigma/E=50/\sqrt{E} \oplus 2\%$  is used.

These results clearly indicate a strong dependence on the performance of the detector despite the enormous QCD background level and the presence of minimum bias events.

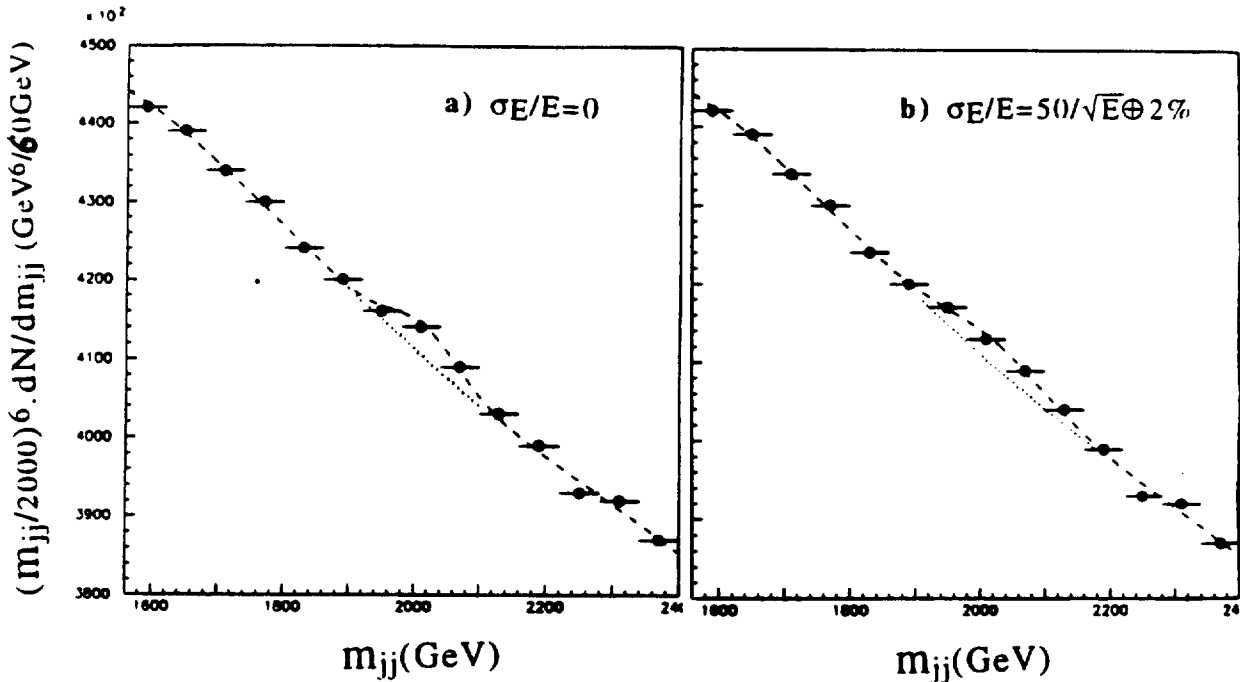


Fig. 13 - Sum of the reconstructed signal and QCD background mass spectrum around the expected 2Tev mass Z' boson for an integrated luminosity of  $10^5 \text{ pb}^{-1}$ . The vertical axis presents the number of events with a 30GeV wide mass bin weighted by the factor  $(m/2000)^6$ . The full line is the combined fit to the expected QCD background and the signal described by three parameters as explained in the text. The dashed line represents the background contribution only. The detector applied has a hadronic energy resolution of (a)  $\sigma/E=0$ , (b)  $\sigma/E=50/\sqrt{E} \oplus 2\%$ .

\*The values obtained without any experiment simulation analysing the signal alone (see results on table 7) were:

-  $\sigma/E=0$ :  $\sigma_m/m = 2.6\%$ ;  $S/\sqrt{B} = 7.6$

-  $\sigma/E=50/\sqrt{E} \oplus 2\%$ :  $\sigma_m/m = 3.4\%$ ;  $S/\sqrt{B} = 7.4$

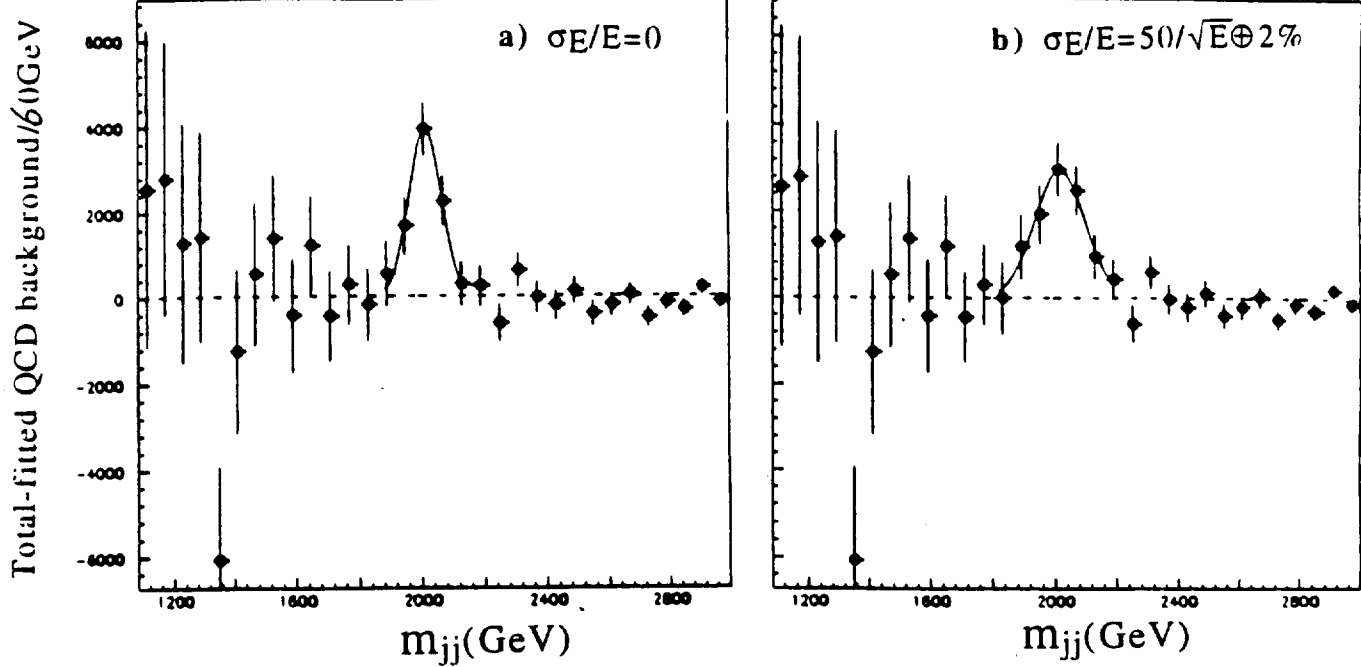


Fig. 14- The dijet mass distribution in the region around the expected 2Tev mass  $Z'$  boson for an integrated luminosity of  $10^5 \text{ pb}^{-1}$  after subtraction of the fitted QCD background. The fit was performed with a single gaussian function with three free parameters  $m_{Z'}$ ,  $\sigma_m$ ,  $N$ , see details on text. The detector applied has a hadronic energy resolution of (a)  $\sigma/E=0$ , (b)  $\sigma/E=50/\sqrt{E}\oplus 2\%$ .

$\sigma/E$ of the detector	parameters of the fit				
	$\mu_{Z'}$	$\sigma_m$	$N$	$\sigma_m/m$	$S/\sqrt{B}$
0	2015	51.5	3910	2.6%	6.8
$50/\sqrt{E}\oplus 2\%$	2016	81.7	2990	4.0%	6.5

Table 8- Characteristics of the curve obtained when the summed dijet mass distribution in the region around the expected 2Tev mass  $Z'$  boson was subtracted by the fitted QCD background. The fit was performed with a single gaussian function with three free parameters  $m_{Z'}$ ,  $\sigma_m$ ,  $N$ , see details on text. The sixth column gives the statistical significance. The detector applied has a hadronic energy resolution of  $\sigma/E=0$  or  $\sigma/E=50/\sqrt{E}\oplus 2\%$ .

## 6- Conclusions

Jets are expected to be a dominant fraction of the information of the physics processes at the LHC experiments, but they also appear to be the main source of the background. In consequence the detection of the  $Z'$  boson in the jet decay mode is a

very difficult task. A simulation of a real experiment was done taking into account the major factors present in future experiments at LHC that can affect the observability of the signal, i.e, the effect of the jet algorithm applied, the presence of minimum bias events, the effect of the energy resolution of the hadronic calorimeter.

The main conclusions of this study are the following:

- As it was already demonstrated in a real hadron collider experiment (UA2/CERN) for the detection of the  $WZ$  pair, the multijet spectroscopy method revealed to be a powerful tool in search of the  $Z'$  boson decaying in two jets. The limiting factors are the poor jet mass resolution and the enormous QCD background levels still remaining after optimization cuts with respect to the signal ( $S/B-10^{-3}$ ).
- This study imposes to work at high luminosities to be able to detect the  $Z'$  boson in the jet decay mode. A maximum mass limit of 3-4 TeV is found. If a  $W'$  would be produced in the same mass range as the  $Z'$  the signal would increase by a factor of 3 (leaving the  $B$  unchanged) and the mass limit of detectability at high luminosity would increase to 4TeV.
- The ideal mass resolution of 1.3% dictated by the natural width of the expected  $Z'$  boson considered ( $m_{Z'}=2\text{TeV}$ ,  $\Gamma_{Z'}=63\text{GeV}$ ) is degraded by a factor of ~2 when a jet algorithm is applied and the minimum bias events are added to the signal, the first effect dominating over the pileup effect. The mass resolution was optimized with the appropriate energy threshold and restrictions for the cone size used for the energy collection. The additional application of a hadronic calorimeter with a crude energy resolution of  $50/\sqrt{E} \oplus 2\%$  produces a final mass resolution of 4.0%, worse by a factor of 3 with respect to the 1.3% ideal value. The energy resolution of the hadronic calorimeter, namely the constant term plays an important role on the degradation of the mass resolution of the  $Z'$  boson signal at the energy range studied, from 1 to 5 TeV.

For this channel a jet energy resolution of  $50/\sqrt{E} \oplus (2-3)\%$  is adequate, but will be a challenge for hadronic calorimeters.

- The sensitivity to possible signals from the  $Z'$  gauge bosons in the jet decay mode is presented in fig. 15 (▼ dots). There is shown the ratio of the expected rate for a specific model to the extended Standard Model ( $\Gamma_{Z'}$  is assumed to increase

linearly with  $m_{Z'}$ ) as a function of the  $Z'$  mass, for a discovery limit of  $5\sigma$  and an integrated luminosity of  $10^5 \text{ pb}^{-1}$ . If other models with a large  $\sigma \cdot B$  would be considered (as alternative left-right symmetric model) [1], the detection limit would increase.

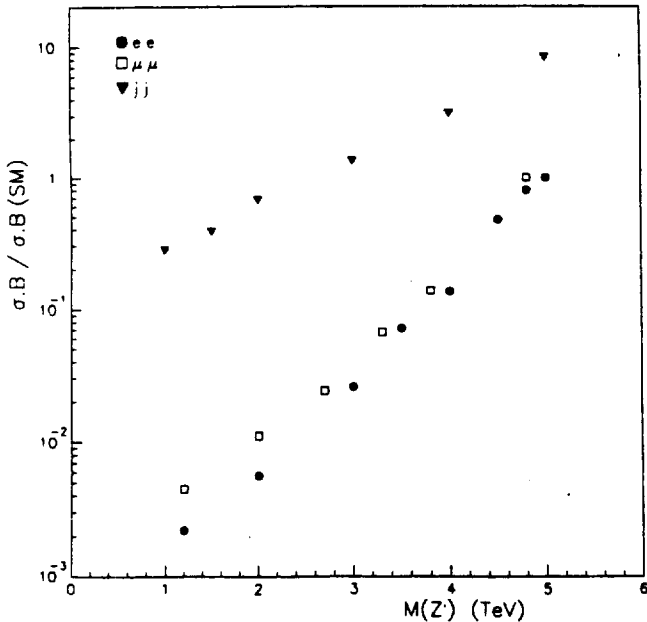


Fig. 15- Discovery limits for  $Z' \rightarrow e^+e^-$ ,  $\mu\mu$ , and  $jj$  considering  $5\sigma$  limits and an integrated luminosity of  $10^5 \text{ pb}^{-1}$  [8].

For completeness is also presented in fig. 15 the case for  $Z'$  decays to electron pairs and muon pairs [8]. The best sensitivity is achieved through the  $Z' \rightarrow e^+e^-$  channel. The other channels, if observed, will provide useful information on the  $Z'$  couplings and possibly asymmetry measurement.

## References

1. *F. del Aguila et. al.*, Proceedings of the LHC workshop, CERN 90-10, ECFA 90-133, VOL. II, pag 686, Oct. 1991.
2. *P. Camarri et. al.*, Proceedings of the LHC workshop, VOL. II, pag 704, Oct. 1991.
3. *J. Pansart*, Proceedings of the LHC workshop, VOL. II, pag 709, Oct. 1991.

4. *P. Bagnaia*, Proceedings of the workshop on physics at the future accelerators, La Thuile, Italie, pag. 181, 7-10 Jan. 1987.
5. *T. Stostrand*, Int. J. Mod. Phys. A3(1988)75.
6. *J. Collas et al.*, Proceedings of the LHC workshop, VOL. I, pag 370, Oct. 1991.
7. *J. Alitti et al.*, Z. fur Physik C 49 (1991) 19.
8. ATLAS LOI, CERN/LHCC/92-4, October 1992.

### **Acknowledgments**

We would like to acknowledge Daniel Froideveaux from providing some of the generated events used, for his useful discussions and constant help. We also thank the summer student J. Luc Perrin for his help in the software modifications in the early phase of this study.